Axonal Damage in Multiple Sclerosis

van der Star, B.J.

2014

document version
Publisher's PDF, also known as Version of record

CHAPTER 3

Differential Immune Responses of White and Grey Matter-Derived Microglia: Relevance for Axonal Damage and Inflammation in Leukocortical Lesions in Multiple Sclerosis

BJ van der Star*, M Olah*, N Papaloukas, D Raj, M Meijer,
N Brouwer, BJL Eggen, KPH Biber, W Gerritsen, C Beyer,
M Kipp, P van der Valk, HWGM Boddeke and S Amor

* These authors contributed equally

Submitted

Abstract
In multiple sclerosis (MS), activated microglia and macrophages have been linked to axonal damage that underlies neurodegeneration and progressive disease. This is exemplified by the finding that cortical grey matter (GM) lesions are characterised by less pronounced microglia activation and lymphocyte infiltration compared to white matter (WM) lesions. Such differences are clearly highlighted by leukocortical lesions that extend across the WM and GM offering an opportunity to examine differences in WM and GM microglia activation in one lesion. So far, dissection of microglia responses in MS has been hampered by an insufficient understanding of factors that trigger activation. Here we have examined leukocortical lesions in people with MS with respect to microglia activation, degree of axonal damage and phagocytosis of neuronal debris. To examine factors that may underlie the differential activation of microglia in the WM and GM *in vitro* studies were performed with mouse microglia. Our studies reveal a clear difference in the degree of microglia activation in the WM and GM of leukocortical lesions that correlated with the extent of axonal damage. Phagocytosis of neuronal debris was more frequent in the WM compared to the GM, but in both regions phagocytosis was associated with axonal damage. Morphometric analysis and gene array studies of mouse microglia showed significant differences between WM and GM-derived microglia in mice. In particular, expression of genes within the Toll-like receptor pathway as well as those associated with antigen processing and presentation pathways were significantly enriched in microglia derived from the WM. On the contrary, direct application of neuronal debris into the corpus callosum or cortex of mice induced profound and comparable inflammation in both regions.
In summary, our data show that microglia activation is reduced in the GM region compared to the WM region of leukocortical MS lesions despite the degree of axonal damage. That we also show a strong differential expression of immune-related genes in WM and GM-derived microglia in mice may explain the differences in microglia activation in the WM and GM in leukocortical lesion in MS.

Introduction
Multiple sclerosis (MS) is a common disease of the central nervous system (CNS) of which demyelination and neurodegeneration are pathological hallmarks. Most research on MS has been performed on the demyelinating part of the disease notwithstanding that the strong neurodegenerative component contributes to the neurological disabilities seen in patients (1). Despite the correlation between inflammation and axonal damage in white matter (WM) MS lesions, the mechanisms contributing to neurodegeneration in MS are largely unknown (2-5). Proposed neurodegenerative mechanisms include chronic demyelination (2, 6), macrophage derived reactive oxygen and nitrogen species (7) and mitochondrial dysfunction (8). In addition, it is suggested that demyelinated axons are more vulnerable to the inflammatory microenvironment containing proteolytic enzymes, oxidative products, cytokines and free radicals, and thereby more susceptible to damage (2, 9). Neurodegeneration could also develop through autoreactivity to neuroaxonal antigens and subsequently targeting of axons, which has been shown in several other neurological disorders (9). Evidence for similar mechanisms in MS comes from antibodies and T cells direct to neuroaxonal antigens as well as axon-reactive B cells in the cerebrospinal fluid (CSF) in people with MS (10-14). It is shown that direct damage to axons, indicated by axonal end bulbs and myelin sheaths devoid of axons, occurs after immunisation with the neuronal cytoskeletal protein

neurofilament light (NF-L) in mice (15, 16). We show phagocytosis of neuronal proteins in MS lesions and an association between phagocytosis, inflammation and the extent of axonal damage in WM MS lesions (17). Although this might indicate a mechanism for damage to axons in the WM, the degree of inflammation, indicated by the number of human leukocyte antigen (HLA)-DR$^+$ cells, is present to a lesser extend in the grey matter (GM) of MS lesions (18). Furthermore, it is shown that extensive axonal damage is present in GM MS lesions, although it contains six times less the amount of CD68$^+$ microglia/ macrophages and 13 times less the number of CD3$^+$ lymphocytes (19).

It is suggested that microglia residing in the WM exist at a higher basal level of activation under physiological conditions compared to microglia residing in the non-myelinated regions of the CNS (20). Supporting this hypothesis, the number of HLA-DR$^+$ microglia and/or the cellular expression level of this molecule in humans, monkeys, dogs and rats under physiological conditions is higher in the WM (corpus callosum, capsula interna) than in the GM (cerebral cortex) (21-27). Moreover, microglia residing in the WM of the forebrain, but also microglia of the spinal cord, are more affected by the ageing related increase in the basal level of activation than their GM counterparts (23, 26, 28). These are indications that microglia residing in the WM and GM of the CNS are phenotypically different, which might be important in the development of leukocortical MS lesions. Therefore, our aim was to study both the WM and GM of leukocortical MS lesions and correlate inflammation, axonal damage and phagocytosis of neuronal debris between those areas. To study microglia in more detail and in a standardised fashion, we investigated morphology, gene expression and functionality *in vitro* in acutely isolated microglia from the corpus callosum and cortex from mice.

Here we report that inflammation was significantly increased in the WM compared with the GM of leukocortical MS lesions, but this was not the case for axonal damage. In WM and GM microglia from mice we observed striking differences regarding the morphology and show substantial heterogeneity at the transcriptome level. Among the differentially expressed genes were transcripts involved in both the innate and adaptive immune system. Microglia from mice derived from the corpus callosum and cortex were to be significantly distinct at the functional level e.g. phagocytic capacity of labelled bacterial particles. Furthermore, stereotactic injection of neuronal rat debris in mice resulted in similar microglia activation in the WM and GM.

Our results indicate that the differences observed in the activation status of microglia derived from the WM compared to the GM may explain the axonal damage that occurs without apparent inflammation in the GM in people with MS.

Materials and methods

Human autopsy tissue

Human tissues were collected from donors with informed consent and by approval of local legal and ethical regulations in collaboration with the Netherlands Brain Bank (protocol 514). Paraffin blocks were used from post-mortem brain material of clinically defined people with MS. MRI-guided sampling of the CNS was used to identify the lesions (29, 30).

Animals

Young adult (8 weeks old) C56BL/6 male mice were purchased from Harlan. Three independent experiments were performed for each assay unless mentioned otherwise.

For stereotactic studies C57BL/6 female mice (11 weeks old) were obtained from Charles River (Germany). Pregnant Sprague-Dawley rats were purchased from Charles River (Germany). Animals were housed and monitored consistent with the principles of the ARRIVE guidelines and were given access to food and water *ad libitum*. All procedures were performed in accordance to appropriate Review Board for the Care of Animal Subjects of the district government under the recommendations of the Federation of European Laboratory Animal Science Associations i.e. Dutch Animal Ethics Committee (PA 13-01) and the German Review Board for the Care of Animal Subjects of the district government (North Rhine-Westphalia, Germany).

Table 1. Patient details

Patient	Gender	Age of death	MS type	Disease duration (years)	PMD h:m	Cause of death
1	F	40	PP	14	7:00	Dehydration
2	F	41	SP	Unknown	8:25	Natural causes
3	F	66	Unknown	Unknown	6:00	Unknown
4	M	51	SP	Unknown	11:00	Unknown
5	F	60	Unknown	10	10:40	Euthanasia
6	F	50	Unknown	Unknown	7:35	Euthanasia

F, female; M, male; PP, Primary Progressive; SP, Secondary Progressive; PMD, post mortem delay.

-

Immunochemistry

Human wax sections were deparaffinised in xylene and rehydrated using descending grades of ethanol. Endogenous peroxidase was blocked using 0.3% H_2O_2 in phosphate buffered saline (PBS) for 30 min. After washing, heat-mediated antigen retrieval was applied in 0.1 M citric acid buffered solution (pH 6.0). Primary antibodies were incubated overnight at room temperature in antibody diluent (Immunologic). Microglia and macrophages were identified with the monoclonal antibody (mAb) to HLA-DR (mouse, clone LN3, 1:100; eBiosciences) and myelin was detected with a mAb to proteolipid protein (PLP, mouse, clone PLpc1, 1:500; Serotec, without antigen retrieval). The sections were subsequently washed and incubated with the secondary Envision polyclonal goat antibody directed to mouse/rabbit conjugated with horseradish peroxidase (HRP, Dako, Denmark). After washing, the enzyme was visualised by incubation with the chromogen 3,3'3-diaminobenzidine (DAB) (Dako). Nuclei were visualised with haematoxylin.

To identify leukocortical lesions both PLP and HLA-DR expression were performed on single sections. First, the sections were treated as described above except that heat-mediated antigen retrieval was applied with Tris-EDTA (pH 9.0). After washing, the sections were simultaneously incubated with the primary antibodies to PLP and HLA-DR. After washing, the secondary goat anti-mouse IgG2a-HRP and goat anti-mouse IgG2b-AP (alkaline phosphatase, both 1:250; Southernbiotech, AL) were applied together for 1 h. The HRP enzyme was visualised using 3-amino-9-ethyl-carbazole (AEC) and the AP enzyme with Fast Blue (FB) chromogen.

To investigate the relationship between activated microglia/macrophages and axonal damage or neuronal cell bodies double staining was performed on paraffin sections by consecutive staining. First, sections were incubated overnight with the primary antibody mAb to amyloid precursor protein (APP, mouse, clone 22C11; 1:1,600; Millipore) or non-phosphorylated NF-H (mouse, clone SMI32R, 1:100; Covance) followed by incubation with the secondary antibody Envision goat anti-mouse/rabbit-HRP. The enzyme was visualised using incubation with AEC. Next,

heat-mediated antigen retrieval with citrate was applied a second time prior to incubation with primary mAb to HLA-DR for 1 h at room temperature. After washing, the second secondary mAb goat anti-mouse IgG2b-AP was applied. Next the sections were washed and FB was used to visualise the phosphatases.

Quantification of inflammation and axonal damage in leukocortical MS lesions
To quantify axonal damage and inflammation in leukocortical MS lesions the border, the rim and the centre of the WM and GM of the leukocortical lesions were identified. The GM was identified by the line of neuronal cell bodies as identified with the mAb to non-phosphorylated NF-H. The edge of the demyelinated lesions defined the rim and the centre was the area between the rim and the border between the WM and GM (Fig. 1). On average, nine photographs of the WM or GM lesion area were taken at 200 x magnification with a Leica DM4000B microscope with Leica DC500 camera to quantify the number of HLA-DR$^+$ cells and axonal damage per mm^2.

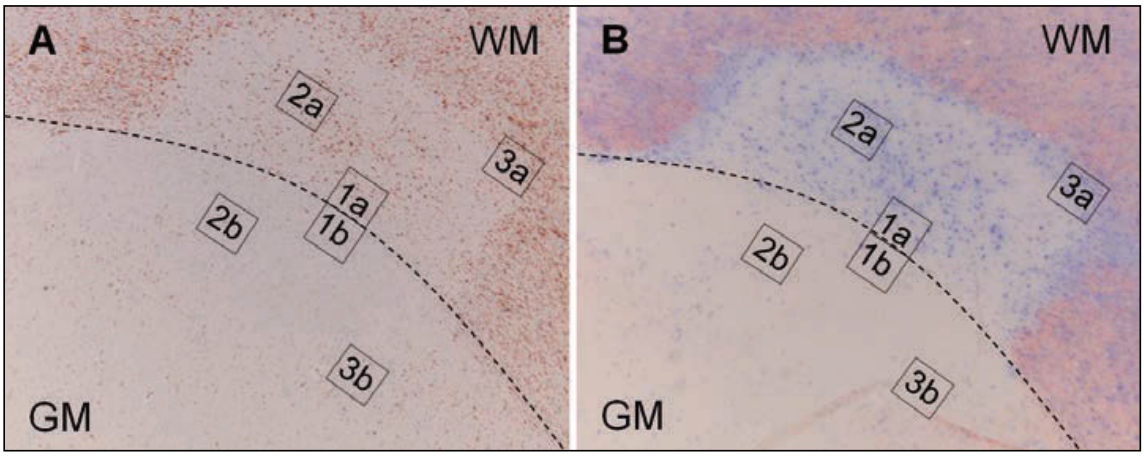

Figure 1. Activated HLA-DR$^+$ cells dominate the white matter region of leukocortical MS lesions. A*) A representative leukocortical lesion reveals high numbers of HLA-DR$^+$ cells in the WM region compared to the GM.* ***B****) Extensive demyelination as shown by staining for PLP (red) in the active part of the WM (HLA-DR, blue). The dotted line represents the border of the WM and GM. The region markers 1a and b represent the region of interest (ROI) on the border of the WM (1a) or GM (1b). ROI 2a and b depicts the centre of the WM part of the lesion (2a) and GM part (2b). ROI 3 represents the rim of the lesion in the WM (3a) or GM (3b).*

Quantification of phagocytosis in leukocortical MS lesions
Due to the low frequency of phagocytosis of neuronal debris (17), the number of HLA-DR$^+$ cells containing APP$^+$ structures was quantified in the total WM or GM lesion area of the leukocortical lesions using light microscopy. Subsequently, phagocytosis of APP$^+$ structures was related to the average number of APP$^+$ ovoids per mm^2 in the WM or GM as well as the average number of HLA-DR$^+$ cells per mm^2 in the WM or GM from the photographs as described above.

Morphometry analysis of mouse microglia
For quantitative analysis of the morphology of WM and GM microglia, immunohistochemistry was performed on brain sections of young adult mice against a microglia marker Iba1. In brief, animals were transcardially perfused with saline under pentobarbital anesthesia followed by 4% paraformaldehyde (PFA). Brains were post-fixed for 24 h, equilibrated in 20% sucrose solution and cryosectioned at 50 μm thickness. Free floating brain sections were blocked with

5% normal goat serum in PBS and subsequently incubated with primary antibody (rabbit anti-Iba1, Wako) for 72 h at 4°C. Primary antibody was then labelled using Cy3-coupled goat anti-rabbit secondary antibody (Jackson Immuno Research). Sections were mounted and coverslipped with Mowiol (Calbiochem). Confocal images of WM and GM microglia were made with a 63 x objective mounted on a Leica SP2 confocal laser scanning microscope. Confocal images were deconvoluted with Huygens Professional imaging software package (SVI). The 3D reconstruction and morphometric analysis of the cells was achieved with the Filament Tracer function of Imaris 7.0 software (Bitplane).

Isolation of primary microglia

Mice were sacrificed by transcardial saline perfusion under inhalation anaesthesia with 4% isoflurane/ 0.4% O_2/ 0.4% N_2O. Brains were isolated and kept in ice cold dissection medium (Hank's buffered salt solution (HBSS) containing 0.6% glucose and 15 μM HEPES buffer (all from Gibco, The Netherlands)). The forebrain was cut into three approximately 1.5 mm thick coronal sections. Coronal sections were further dissected into white (corpus callosum) and grey (cerebral cortex) matter on ice. From the collected tissue, microglia were isolated at high purity (> 98%) using a discontinuous Percoll gradient (31). All steps of the isolation were performed at 4°C. Briefly, the tissue was transferred into a bouncing tissue homogeniser and mechanically dissociated. The homogenate was further homogenised with four Pasteur pipettes of decreasing diameter until a single cell suspension was attained. The cell suspension was then filtered through a 70 μm cell strainer, washed with dissection medium and pelleted by centrifugation. The pellet was resuspended in 75% Percoll, overlaid with 25% Percoll and finally with PBS. The density separation was achieved by centrifugation of the discontinuous Percoll gradient in a swinging bucket centrifuge at 800 *g* for 25 min. Microglia were then collected from the 75%-25% Percoll interface, washed with PBS and pelleted by centrifugation. The cell pellet was resuspended in culture medium (Dulbecco's modified eagle medium (DMEM) containing 5% fetal calf serum (FCS), 1% penicillin/streptomycin and 1% sodium-pyruvate, all from Invitrogen) for the phagocytosis assay as described below. In case of flow cytometric analysis of surface expression markers, the pellet was resuspended in PBS. For total RNA extraction for further gene expression analysis, the pellet was lysed in lysis buffer. In some cases (e.g. gene expression analysis), before the final centrifugation, a small sample of few thousand cells was taken out from the cell suspension to assess the purity of microglia isolation by flow cytometry.

Phagocytosis assay

After isolation, WM and GM microglia were resuspended in culture medium and seeded in 8 well Lab-Tek™ II Chambered Coverglass (Nunc) at a density of 5,000 cells per well. Two hours after seeding, the medium was replaced with culture medium containing 25 μg/mL of pHrodo™ E.coli BioParticles® conjugate (Invitrogen). Cells were subsequently imaged for 18 h with a Solamere Nipkow spinning disc confocal laser scanning microscope mounted on a Leica DM IRE2 inverted microscope equipped with a HC PL APO CS 10 x dry objective, a Stanford Photonics XR/Mega-10I (intensified) CCD camera, and a temperature (37°C) and CO_2 concentration (5%) controlled imaging chamber. To excite the pHrodo dye, a 568 nm laser line of a dynamic Krypton laser was used. A brightfield and a red channel image were acquired every 5 min for each condition ("white" and "grey matter" wells). For both

white and grey matter wells, one field per well, which contained in both cases 20-30 cells was imaged. Multiple cells were selected as regions of interest (ROIs) based on the brightfield images. The intensity of the ROIs in the red channel images was measured in each frame of the entire image stack with the help of an ImageJ plugin (written by K. Sjollema; UMCG-UMIC, Groningen, The Netherlands). The data were plotted as a time versus intensity curve and the time needed to reach half maximum response for each cell was determined in Excel.

Gene expression analysis
Eight biological replicates were used for each condition (WM and GM), each consisting of a pool of three mice. Each sample was tested for purity of microglia preparation with flow cytometry as described below. After the dissection of WM and GM and isolation of microglia, total RNA was isolated with a QiagenRneasy® Micro kit (Qiagen). The amount of isolated RNA was determined with a NanoDrop™ 2000 spectrophotometer. From each sample 25 ng of total RNA was used. The integrity of the RNA samples was confirmed with an Agilent Bioanalyzer automated electrophoresis system using the RNA 6000 Pico LabChip® Kit. The RNA integrity was determined by visual examination of the electropherograms and by the RNA integrity number (RIN). Only samples with RIN> 8 and clear 18S and 28S ribosomal RNA peaks were included in the gene expression study. The RNA was then processed for microarray analysis: copyDNA synthesis, amplification and biotin-labelled copyRNA production were done with an Illumina® TotalPrep™-96 RNA Amplification Kit (Ambion). Subsequently, 750 ng of biotin-labelled cRNA was hybridised to Illumina MouseRef-8 v2.0 bead arrays according to the manufacturers protocol. The bead arrays were then stained with streptavidin-Cy3 and scanned with iScan System (Illumina).

Endotoxemia model
Mice were injected intraperitoneally either with 50 μg LPS/25 g body weight dissolved in saline or with equal volume of saline (control). Eight hours after injection, mice were sacrificed by transcardial perfusion with saline under pentobarbital anaesthesia. Brains were removed from the skull, WM and GM regions were dissected and microglia were isolated from these regions as described above. After isolation WM and GM microglia were analysed by flow cytometry.

Flow cytometry
Isolated microglia from healthy mouse brain or an endotoxemia mouse model were resuspended in PBS and Fc blocked with 1% anti-CD16/32 (eBiosciences) for 15 min, stained for different surface markers (see below) for 20 min, washed with PBS, pelleted with centrifugation and resuspended in PBS for subsequent flow cytometric analysis. During the staining procedure and before analysis, cells were kept on ice. Stained cells were analysed with BD™ LSR II multi-laser flow cytometer. The flow cytometric measurements were evaluated using WinList 6.0 software. The geometric mean fluorescent intensities (MFI) of each measurement were used for statistical analysis.
To determine the purity of microglia preparation, a small sample of the attained cell suspension was stained for CD11b and CD45 together with a live cell marker DRAQ5™ (Biostatus Ltd.). Microglia purity was determined as the percentage of $CD11b^{high}/CD45^{low}/DRAQ5^{+}$ cells (live microglia) among the total $DRAQ5^{+}$ cells (live cells). The microglia purity was routinely above 98%.

For immunophenotyping of mouse microglia cells, the following antibodies were used: phycoerythrin (PE)-coupled rat anti-mouse CD11b (Cat.No. 12-0112), allophycocyanin (APC)-AlexaFluor750-coupled rat anti human/mouse CD11b (Cat. No. 27-0112; discontinued), AlexaFluor700-coupled rat anti-mouse CD45 (Cat.No. 56-0451), fluorescein isothiocyanate (FITC)-coupled rat anti-mouse CD45 (Cat.No. 11-0451), FITC-coupled Armenian hamster anti-mouse CD40 (Cat.No. 11-0402), FITC-coupled Armenian hamster anti-mouse CD80 (Cat.No. 11-0801), FITC-coupled rat anti-mouse CD86 (Cat.No. 11-0862), FITC-coupled rat anti-mouse F4/80 (Cat. No. 11-4801), PE-coupled rat anti-mouse CXCR3 (from R&D, Cat.No. FAB1685P), FITC-coupled rat anti-mouse MHC class II (Cat.No. 11-5321), PE-coupled rat anti-mouse TLR1 (Cat.No. 12-9011), FITC-coupled rat anti-mouse TLR2 (Cat.No. 11-9021), PE-coupled mouse anti-mouse TLR4 (Cat.No. 12-9041). Appropriate isotype controls were used for each staining in a concentration-matched manner. All flow cytometry antibodies (and the corresponding isotype controls) were obtained from eBiosciences, unless mentioned otherwise.

Intracerebral injection of neuronal debris

Neuronal debris was collected from 1 day-old Sprague-Dawley rats cortices following an optimised protocol (Dr. M Witte, VUmc, The Netherlands). Briefly, neopallia were dissected in dissection medium containing HBSS (Gibco), sodium pyruvate (Gibco), 0.1% D-glucose (Sigma-Aldrich) and 10 mM Hepes (Sigma-Aldrich). Cortices were transferred to dissociation medium containing DMEM, 0.25% trypsin, 1 mg/mL DNAse I (all from Gibco), and let dissociated at 37°C. The suspension was diluted in HBSS and filtered through a cell strainer (100 mm, VWR) and centrifuged (500 *g*, 5 min). Subsequently cells were plated in cell flasks coated with 50 μg/mL poly-L-lysine (Sigma-Aldrich). Neurons were cultured in neurobasal medium supplemented with penicillin (100 U/mL), streptomycin (100 mg/mL), 2% B27 and 1x glutamax (all from Gibco). After 1 and 4 d half the culture medium was changed and 10 μM cytosine arabinofuranoside (Sigma-Aldrich) was added to exclude glial cells from the culture. Neurons were cultured for 7 d after which the cells were scraped off and collected in PBS. Concentration was measured using the Bradford assay (Bio-Rad, Germany).

Neuronal debris was injected as described before for myelin debris (18). Briefly, C57BL/6 mice were fixed in a mouse adapter for stereotactic frames (World Precision Instruments). After drilling a small hole in the skull, 0.2 μg of neuronal debris was injected into the respective regions using a 10 μL syringe equipped with a 33 gauge needle (Hamilton Company) with a volume of 6 nL/s by using a Ultra Micro Pump (UMP3, World Precision Instruments). Coordinates for injection were X (-2.2), Y (0.6) and Z (0.8 for cortex and 1.5 for corpus callosum) relative to the anterior bregma. The needle was navigated by a motor-driven stereotactic frame (World precision instruments) utilising StereoDrive software (Neurostar). The injection was carried out within a standardised time frame i.e. ~5 min injection time and 10 min deposition rest in the cortex before the needle continued to the corpus callosum. Subsequently, needle was retracted after 5 min deposition rest in order to prevent potential variations in the effect of shearing forces. At 2 d post-injection, mice were sacrificed by injection with 10% chloralhydrate, perfused with PBS and 4% PFA where after brains were fixed in 4% PFA overnight and routinely processed for paraffin embedding.

Immunochemistry of mouse brain following stereotactic injection
Paraffin embedded brain sections (6 μm) of mice stereotactically injected with neuronal debris from rat were deparaffinised as described above. After blocking endogenous peroxidase (0.3% H_2O_2), antigen retrieval was performed in Tris-EDTA pH 9.0 in a microwave. After cooling, sections were blocked with CleanVision mouse to-mouse block (Immunologic) or 10% normal goat serum (Dako) and subsequently stained with mAbs to NF-L (mouse, clone 10H9, 1:100; made in house) and Iba1 (1:10,000) overnight. After washing, sections were incubated with Envision goat anti-mouse or Envision goat anti-rabbit conjugated with HRP and visualised with DAB chromogen. Nuclei were visualised with haematoxylin.
To localise the injection tract, serial sections were stained with haematoxylin and eosin.
For immunofluorescence, sections were double stained with mAbs to NF-L (1:100) and Iba1 (1:2,000) overnight. After washing the sections, secondary mAbs goat anti-mouse IgG1 Alexa Fluor 594 and goat anti-rabbit IgG Alexa Fluor 488 (Invitrogen) were incubated for 1 h at room temperature. Images were taken on a Confocal microscope (Leica TCS SP1) using a 63 x magnification.

Statistics
Data were analysed in PrismGraph 5.0 and SPSS 12.0.1. Correlations in leukocortical MS lesions were identified using the non-parametric test Spearman rank correlation. To investigate significant differences between two variables, the Student's *t*-test was used for parametric data or the Mann-Whitney U test was used for non-parametric data.
Statistical analysis of the gene expression data was performed in GeneSpring software after normalisation using BeadStudio software (Illumina). Two approaches were applied: 1) with significance testing (*t*-test, Benjamini correction for multiple testing) we determined the genes that were expressed at a significantly different level ($p<0.05$, fold change >1.5) in white and grey matter microglia; 2) with an empirically determined cut-off value (noise level) we determined the genes that were present in either white or grey matter microglia. A functional annotation chart of the differently expressed genes was generated using the DAVID Bioinformatics Resources web application (http://david.abcc.ncifcrf.gov/). Unpaired *t*-test was performed with an asymptotic p value computation. In all cases, p values were considered significant if $p<0.05$ (*); $p<0.01$ (**); $p<0.001$ (***).

Results

Axonal damage is similar in white and grey matter of leukocortical MS lesions
Analysis was performed on 10 blocks from 6 MS patients containing 13 leukocortical lesions (Table 1). The number of HLA-DR^+ cells and APP^+ ovoids in the WM or GM part of the leukocortical lesions was recorded. Significantly more HLA-DR^+ cells were observed in the WM part compared to the GM part of leukocortical lesions ($p<0.0001$, Fig. 2A). In contrast, no difference was observed in the extent of axonal damage, as depicted by the number of APP^+ ovoids (Fig. 2B). Our analysis confirmed a positive correlation between the number of HLA-DR^+ cells and axonal damage in the WM ($r=0.4182$, $p<0.0001$, Fig. 2C) but not in the GM ($r=0.08698$, $p>0.05$, Fig. 2D). This may indicate differences in microglia function in the WM and GM.

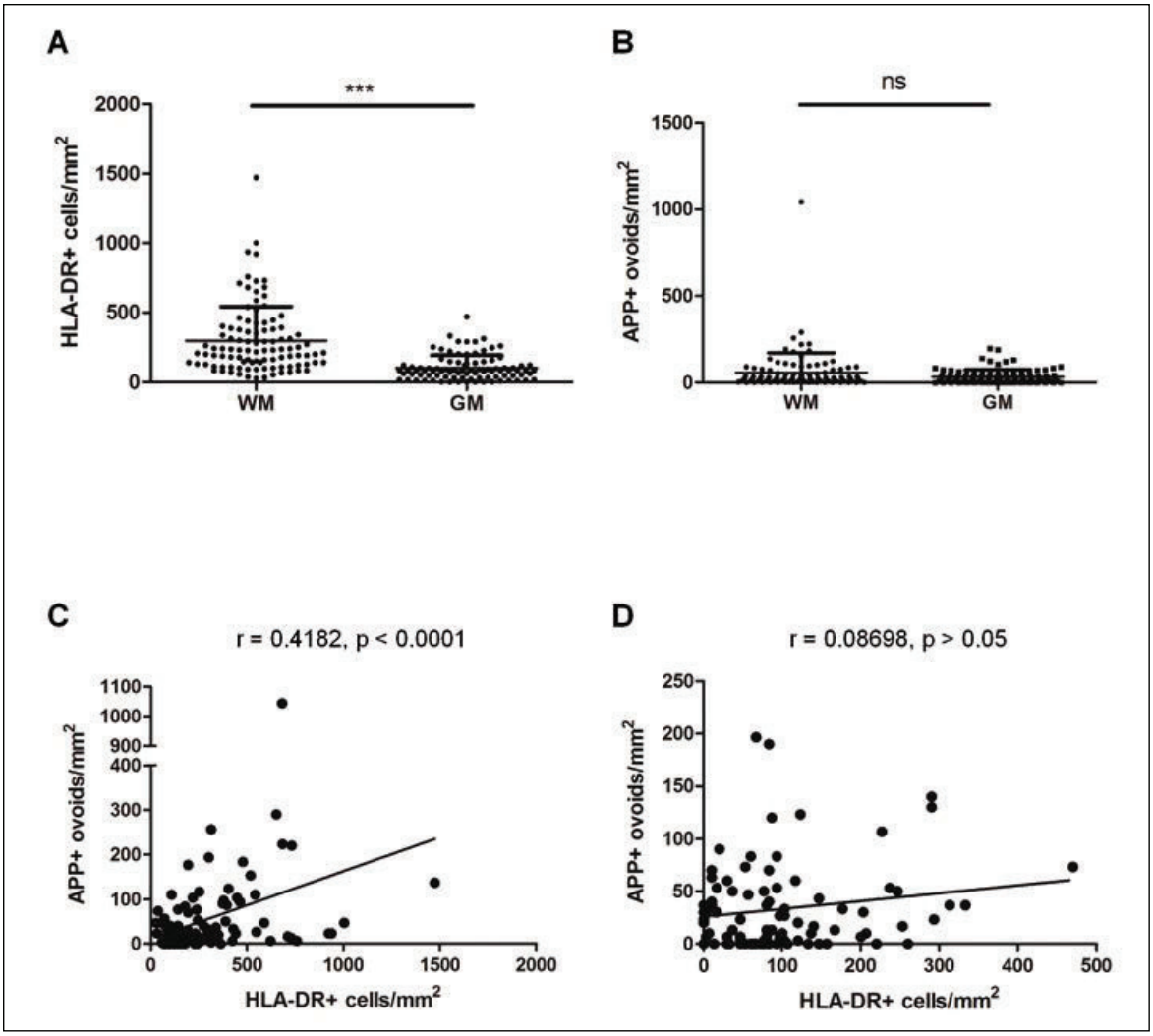

Figure 2. Expression of HLA-DR⁺ cells in leukocortical MS lesions. A*) The numbers of HLA-DR cells in the WM compared to the GM part of leukocortical MS lesions (n=13, p<0.0001, Mann Whitney U test) and (**B**) APP ovoids in the WM compared to the GM (p>0.05, Mann Whitney U test).* ***C****) Correlation between the number of HLA-DR cells and APP ovoids (r=0.4182, p<0.0001) in the WM but not in the GM regions of leukocortical MS lesions (**D**, r=0.08698, p>0.05, Mann Whitney U test).*

Phagocytosis of neuronal debris in leukocortical MS lesions

Since phagocytosis of neuronal antigens is associated with the extent of axonal damage in WM MS lesions (17), we examined phagocytosis of APP⁺ structures in the total WM or GM leukocortical lesion area using a 200 x objective (Fig. 3A). Phagocytosis of APP⁺ structures was more frequently observed in the WM region of leukocortical lesions compared with the GM (Fig. 3B, $p<0.05$, Mann-Whitney U test). We then investigated the relation between the degree of phagocytosis and the number of HLA-DR⁺ cells and/or axonal damage. Although we did not observe an association between phagocytosis and number of HLA-DR⁺ cells in the WM ($r=0.3504$, $p>0.05$) nor the GM ($r=0.4228$, $p>0.05$, data not shown), the number of HLA-DR⁺ cells containing APP⁺ structures correlated with axonal damage in both the WM (Fig. 3C, $r=0.8026$, $p<0.001$) and the GM (Fig. 3D, $r=0.5981$, $p<0.05$).

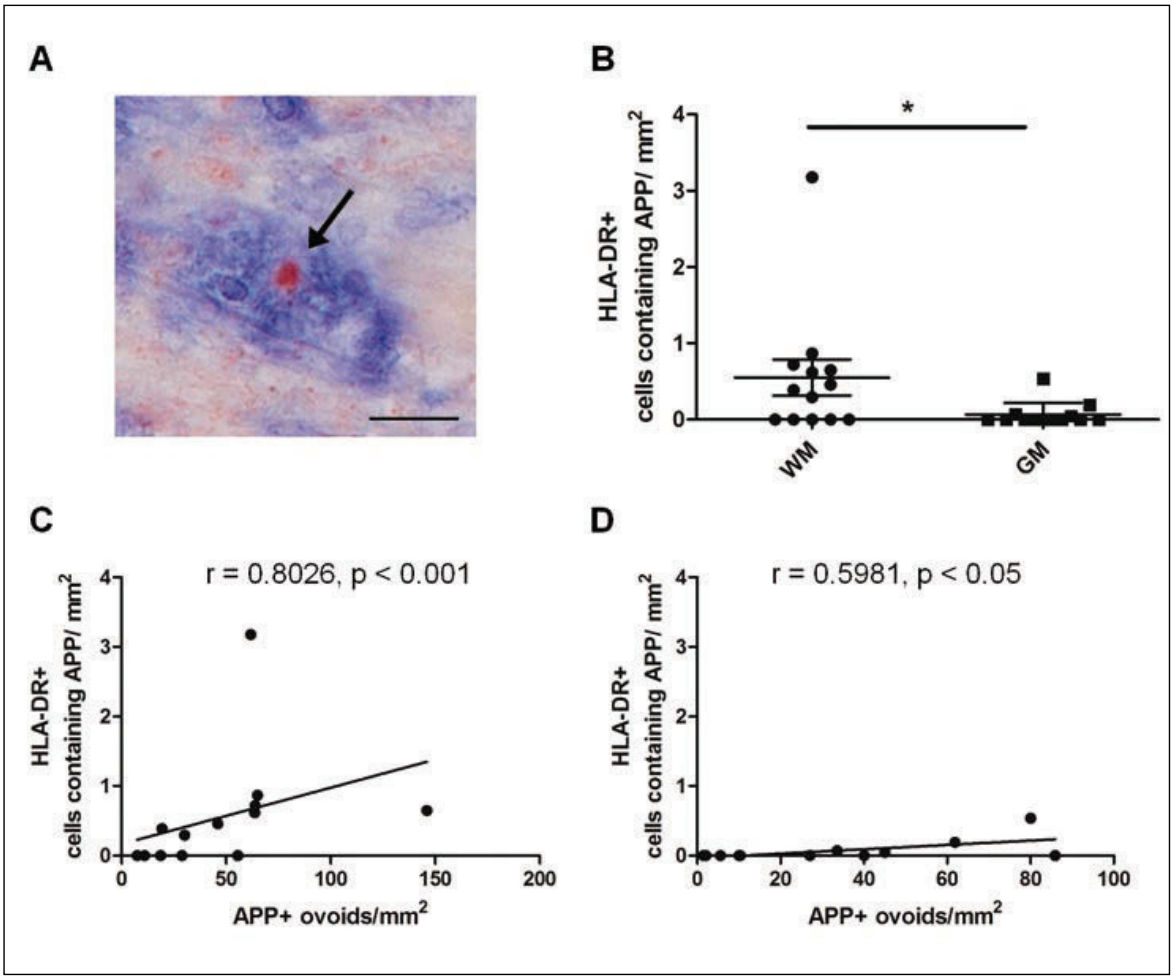

Figure 3. Phagocytosis of APP⁺ structures by HLA-DR⁺ cells correlates with axonal damage in leukocortical MS lesions. A*) Phagocytosis of APP structure (red) is seen by an HLA-DR cell (blue) in the WM.* ***B****) Phagocytosis of APP structures by HLA-DR cells is more frequently observed in the WM region compared to the GM (p<0.05, Mann Whitney U test). The number of HLA-DR cells containing APP correlates with axonal damage in the WM (****C****, r=0.8026, p<0.001) and in the GM (****D****, r=0.5981, p<0.05). Scale bar in (A) =15 µm.*

Microglia from white or grey matter are distinct subpopulations according to their morphology

Numerous studies have described morphological differences between microglia residing in WM and GM based on visual examination. In this study, we investigated morphological differences between cortical (Fig. 4A) and callosal (Fig. 4B) microglia in mice using a quantitative morphometric method. Each biological replicate (independent experiment) consisted of a pool of three mice in order to obtain a sufficient amount of microglia from the white matter (corpus callosum). Random Iba1⁺ cells were chosen from both regions of the CNS. We mainly focused on the process arborisation of the cells, since the size, spatial arrangement and ramification of their processes are primarily affected when microglia transform from ramified/ resting to activated state. As shown in Figure 4, WM microglia are morphologically different from GM microglia. Quantification analysis showed significant differences in total dendrite length, total processes volume and the number of primary ramification points on their process arborisation (Supp. Fig. 1).

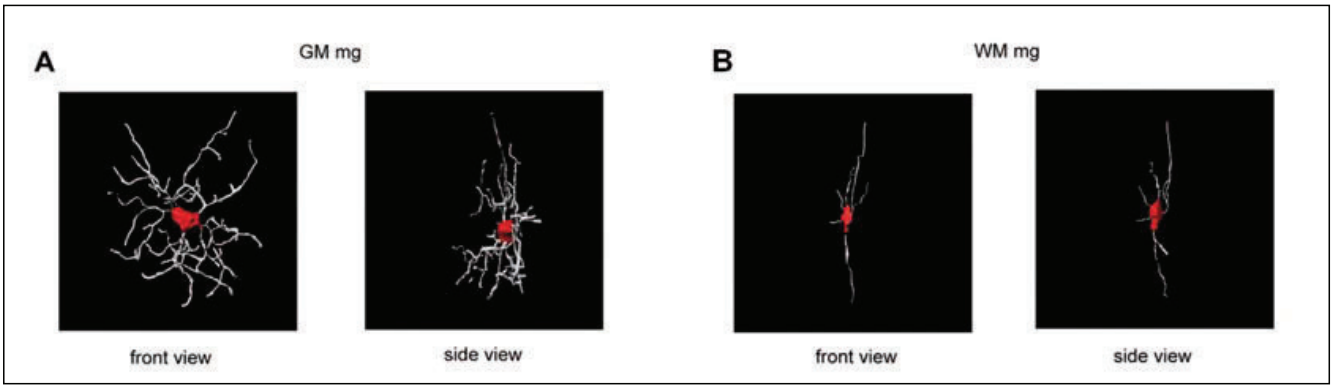

Figure 4. Differential morphology of microglia derived from in the corpus callosum (WM) and cerebral cortex (GM) *using the Filament Tracer function of the Imaris software package. Each biological replicate (independent experiment) consisted of a pool of three mice. Snapshots from the 3D reconstructions of GM (**A**) and WM (**B**) microglia. Front view is perpendicular to the coronal plane, while side view is perpendicular to the sagittal plane. GM mg, grey matter microglia; WM mg, white matter microglia.*

Similar phagocytosis by mouse microglia from white or grey matter

To compare whether WM and GM microglia inherently differ from each other on a functional level, we investigated the rate of phagocytosis of pHrodo-coupled bacterial particles by time-lapse microscopy in acutely isolated microglia from mice (Fig. 5C). The mean intensity across the stack was measured off-line with ImageJ software for each cell and plotted against time to yield the phagocytic curves depicted in Figure 5A. Acutely isolated WM and GM microglia had similar phagocytic capacity (Fig. 5B, n=100 for both WM and GM microglia, three independent biological replicates). In addition, there was no significant difference between WM and GM microglia in respect of the percentage of cells that reached half maximum phagocytosis at any given time point (Fig. 5B).

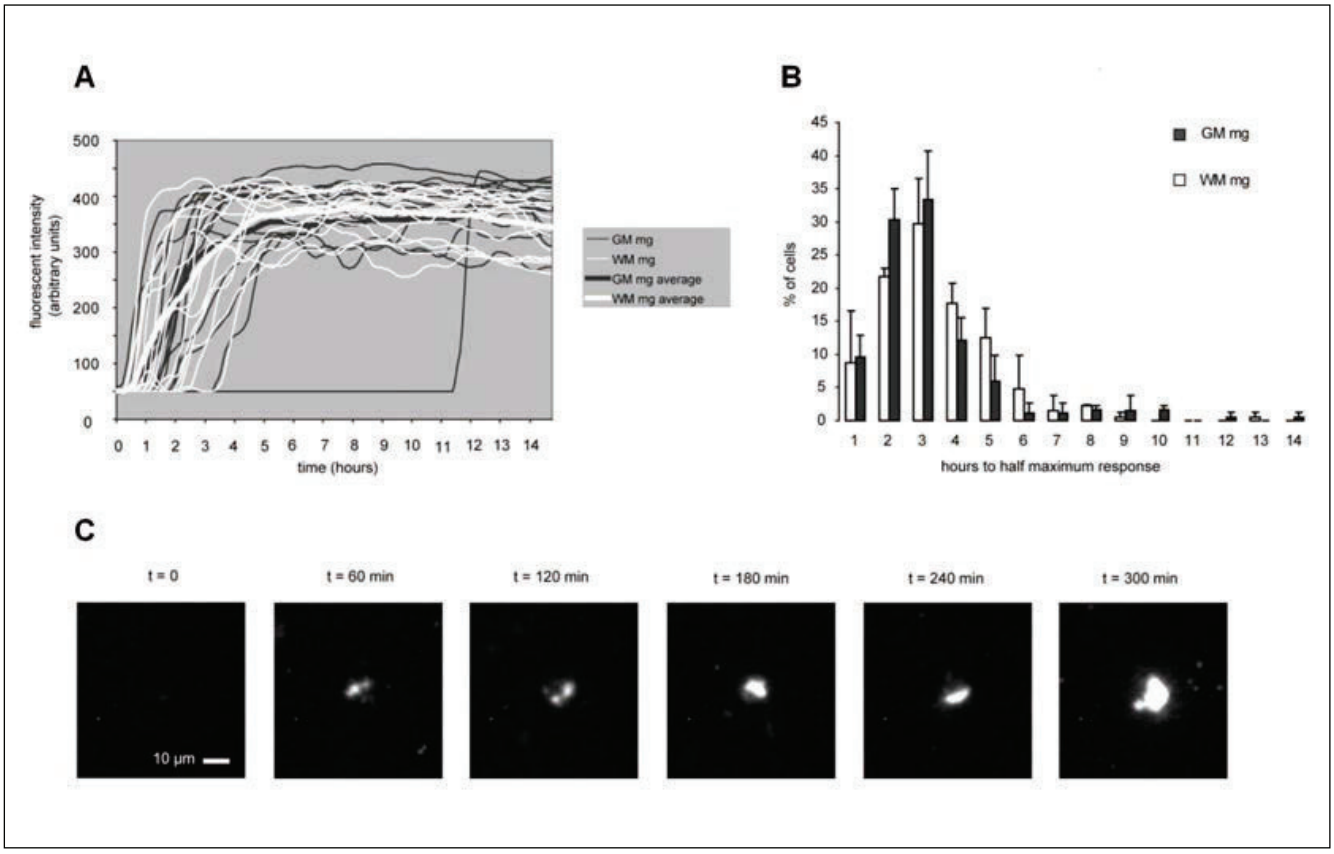

Figure 5. Similarities of functional phagocytosis assay in mouse microglia. A*) Representative graphs of the timelapse measurements of the phagocytosis of the bacterial particles pHrodo by WM and GM microglia (n=100 cells per group).* ***B****) Histogram showing the percentage of cells belonging to the given categories regarding the rate of phagocytosis.* ***C****) Representative photomicrographs from the time-lapse confocal microscopic measurements showing the accumulation of the pHrodo-coupled bacterial bioparticles in microglial phagolysosomes. As seen in the pictures, pHrodo only becomes visible as a fluorescent signal when present in an environment with low pH, such as the lysosomes. GM mg, grey matter microglia; WM mg, white matter microglia. See figure on the previous page.*

Genome wide gene expression analysis of acutely isolated white and grey matter microglia from mice

To investigate the differences in the gene expression pattern between cortex and corpus callosum resident microglia populations, we performed a genome wide gene expression analysis using Illimuna bead arrays. Eight biological replicates were used for each group (WM and GM microglia), each of which consisted of a pool of three to five mice. After normalisation and log2 transformation, the two groups were tested for the presence of significantly differentially expressed genes. We found more than 1,300 genes that were expressed at a significantly higher level in GM than in WM microglia and around 1,200 genes that were expressed at a significantly higher level in WM than in GM microglia (Fig. 6A-B). The fold change difference between the expression levels of WM and GM microglia genes was rarely above fivefold, and the largest difference was less than 20 fold (Fig. 6B). Next the gene lists were submitted to gene ontology analysis using DAVID web-application (http://david.abcc.ncifcrf.gov/) to investigate the identity of the significantly different expressed genes. Several neuroimmunologically-relevant pathways showed to be significantly enriched (modified Fischer Exact p value for gene enrichment analysis/EASE score threshold: 0.05, multiple testing correction: Benjamini) in the differently expressed genes (Fig. 6C-D). Amongst the pathways that were significantly enriched in genes expressed at a higher level in WM microglia (p=3.0E-5, Benjamini=4.8E-3) was the Toll-like receptor signalling pathway. Importantly, as depicted in Figure 6C, the differently expressed genes belonging to this pathway included the receptors (*Tlr1*, *Tlr2*, *Tlr6*, *Tlr4* and *Cd14*), members of the signalling cascade (*Tirap*, *Irak4*, *Traf6*) and the effector molecules (*Tnf*, *Ccl5*, *Ccl4*). Similarly, the pathway of antigen processing and presentation was also showing the trend of being enriched in genes expressed at a higher level in WM microglia (Fig. 6D, p = 1.8E-1, Benjaminin=6.3E-1). Among the significantly differentially expressed genes belonging to this pathway were genes associated with antigen processing and loading of the major histocompatibility molecules with the processed antigen (*Hsp70*, *Ifi30* (*Gilt*), *Ctsb*, *Ctsl*, *Ctss, H2-DM*). Moreover, the genes associated with the major histocompatibility complex I and II and the invariant chain CD74 (*Ii*) were significantly differentially expressed as well (Fig. 6D).

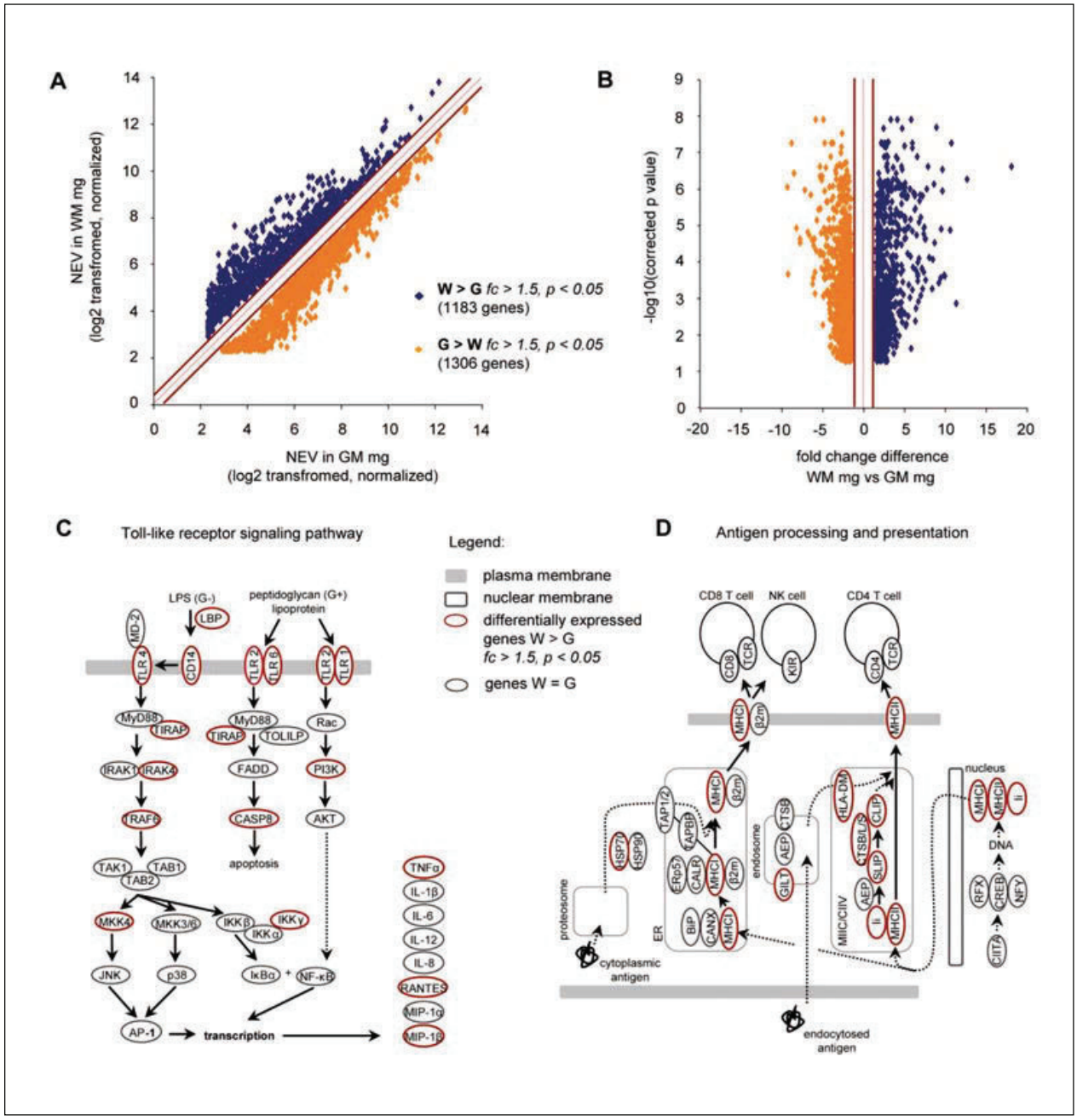

Figure 6. Genome wide gene expression analysis reveals significantly differentially expressed genes in white and grey matter mouse microglia. A*) The scatter plot represents the normalised expression levels of the significantly (corrected p value<0.05) differentially expressed genes between WM and GM microglia (n=3-5 mice per group, 8 replicates). The diagonal red lines represent the cut off value of 1.5 fold difference in expression level.* ***B****) In the volcano plot depicting the significantly (corrected p value <0.05) different expressed genes, the fold change difference between the expression level of a given gene in WM and GM microglia is plotted against the –log10 transformed p value of the particular gene. The vertical red lines represent the cut off value of 1.5 fold difference in expression level.* ***C****) and* ***D****) show example pathways that were significantly enriched in differentially expressed genes between WM and GM mouse microglia. The significantly differentially expressed genes are represented in red ellipses. Pathway analysis was done using DAVID web application. Pathways reconstructed based on KEGG pathway.* ***C****) The Toll-like receptor pathway was significantly enriched in genes that were expressed at a significantly higher level in WM microglia.* ***D****) The antigen processing and presentation pathway was significantly enriched in genes that were expressed at a significantly higher level in WM microglia. FC, fold change; p, corrected p value.*

Immunophenotyping of white and grey matter microglia from mice by flow cytometry
We next investigated the observed differences in gene expression at the protein level using flow cytometry. Surface markers belonging to the two signalling pathways that were significantly enriched in genes expressed at a significantly higher level in WM than in GM microglia were chosen, namely the Toll-like receptor pathway (two independent experiments) and the antigen processing and presentation pathway (three independent experiments). Contrary to our gene expression analysis, we found no differences between WM and GM microglia in respect of the surface expression of selected Toll-like receptors (Figure 7B), MHCII and the co-stimulatory molecules under physiological conditions (SAL histograms in Figure 7C). In accordance with previous reports (31, 32), the above mentioned surface markers were either absent (e.g TLR1, MHCII) or expressed at a low level (e.g. TLR2, TLR4) on microglia in the non-inflamed murine brain. To explore whether the differences observed at the gene expression level translate into dissimilarities in the responsiveness of WM and GM matter microglia upon stimulation *in vivo*, we performed flow cytometric analysis of certain selected activation markers (among others MHCII and the co-stimulatory molecules) of WM and GM microglia isolated from an endotoxemia model. As depicted in Figure 7D, the induction of several activation markers was different between WM and GM microglia. While F4/80, CXCR3 and CD80 were induced to a similar extent in both WM and GM microglia (Figure 7D), there was a three fold stronger induction of CD40 and CD86 in white matter microglia than in grey matter microglia (Figure 7C). Induction of MHCII was also slightly stronger in white compared to grey matter microglia upon peripheral endotoxin challenge (Figure 7C-D).

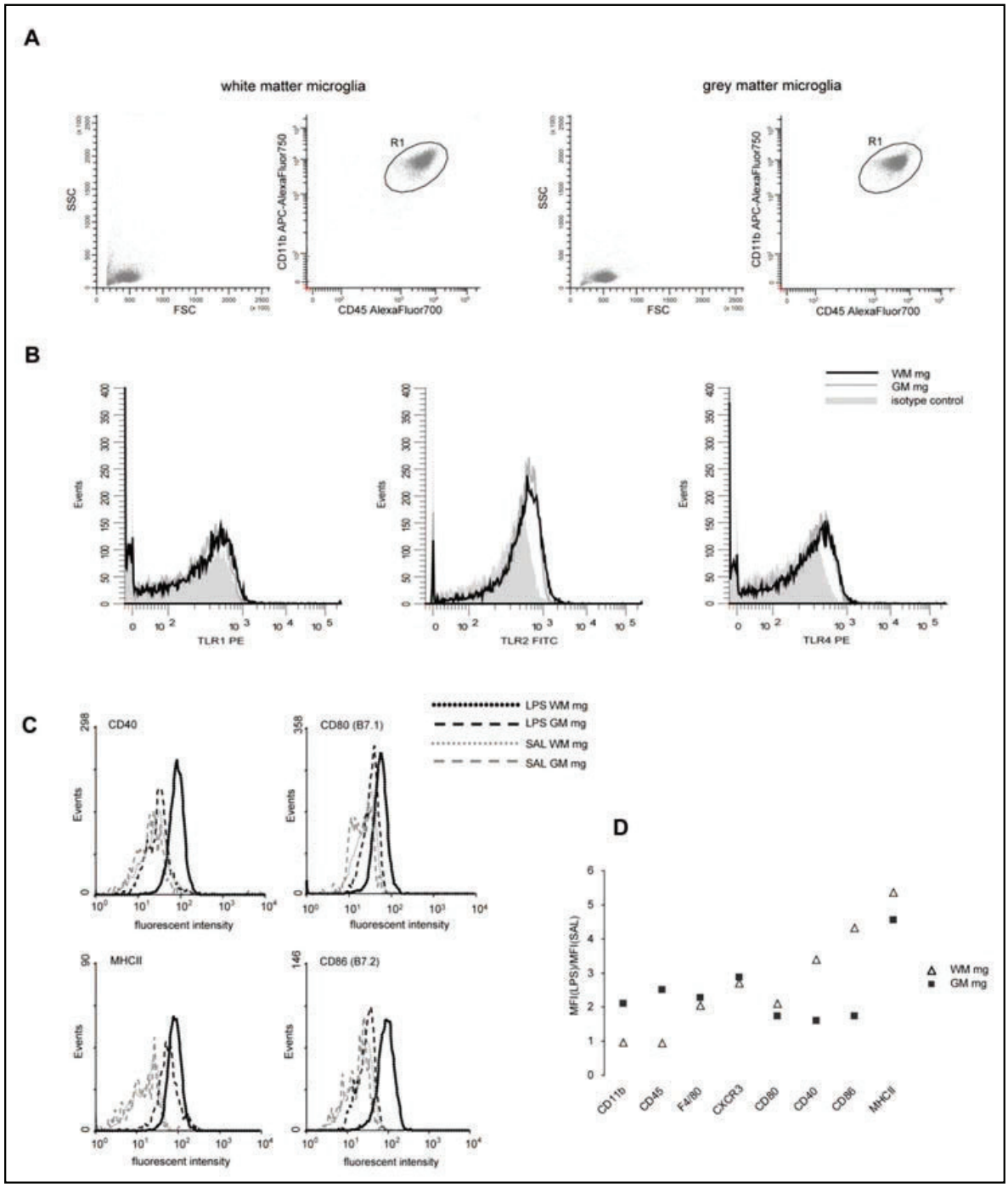

Figure 7. Comparison of the expression levels of Toll-like receptors and certain microglia activation markers on white and grey matter microglia by flow cytometry. A*) Acutely isolated white and grey matter microglia showed the characteristic forward and side scatter (FSC/SSC) profile and the typical CD11b^{high}/ CD45^{intermediate} expression levels. The events within R1 were used for further analysis.* ***B****) TLR2 and TLR4 were expressed at a low level on acutely isolated white and grey matter microglia under physiological conditions, while TLR1 was not present (representative histograms of one out of two independent experiments).* ***C*** *and* ***D****) Induction of the expression of certain inflammatory markers on white and grey matter microglia upon systemic LPS challenge. Under physiological conditions most of the markers were expressed at a comparable level between white and grey matter microglia. In the endotoxemia model, some markers (such as CD86, CD40 and MHCII) were induced to a greater extent in white matter microglia than in grey matter microglia. Histograms show representative measurements of one out of three independent experiments. MFI, mean fluorescent intensity; WM mg, white matter microglia; GM mg, grey matter microglia; LPS,* lipopolysaccharide *challenge; SAL, saline injected.*

Activation of microglia in mouse brain following injection with neuronal debris in the absence of myelin

Recently, Clarner and colleagues suggested that the low degree of microglia activation in the GM is a result of less myelin present in the GM region (18). We observed a similar degree of axonal damage in the WM and GM part of leukocortical MS lesions, but clear differences in inflammation. Therefore, we investigated whether the presence of neuronal debris would result in microglia activation in both WM and GM. Neuronal debris derived from rat was injected stereotactically in mice (n=2) followed by immunochemistry. To compare microglia activation in the GM and WM, neuronal debris was injected in the cortex followed by injection in the corpus callosum. In both areas injection of neuronal debris led to microglia activation indicated by staining with anti-Iba1 (Fig. 8). Neuronal debris was also present. Using laser scanning confocal microscopy, phagocytosis of neuronal antigens in the area of injection was observed by Iba1^{+} cells (Fig. 8 H-I), in both the WM and GM. These results indicate that in mice, there seem to be no differences in the ability of HLA-DR+ cells in the WM and GM to respond to acute injury.

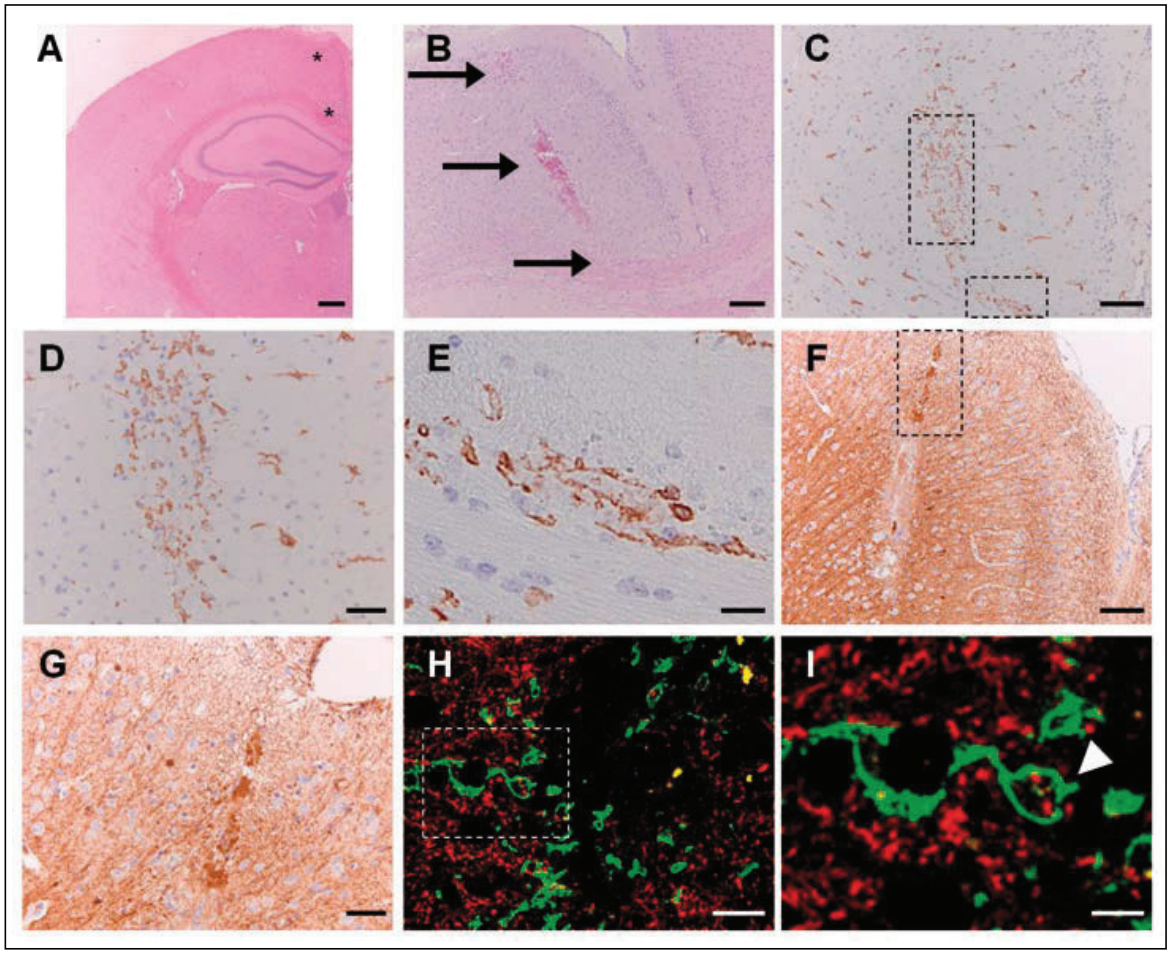

Figure 8. Microglia activation following neuronal debris injection in mouse brain. A) *Coronal overview of the region where stereotactic neuronal debris application has been performed (indicated by stars). The injection channel indicated by the arrows was identified using haematoxylin and eosin stain (**B**). **C**) Identification of microglia expressing Iba1 in the injection channel showing the cortex (upper square and **D**) and corpus callosum (lower square and **E**). Neuronal debris as identified with NF-L at the area of injection (**F**). **G**) Enlargement of dotted square in (F). **H** and **I**) Confocal microscopy shows Iba1 microglia (green) containing neuronal antigens (NF-L, red, arrowhead) in the cortex at the injection site. Scale bars=100 µm (A/C/F), 200 µm (B), 50 µm (D/G), 25 µm (E), 30 µm (H), 10 µm (I).*

Discussion

In MS, GM lesions have only become extensively studied in the last decade since axonal damage correlates with clinical disability (1). In particular, leukocortical lesions are interesting because of the ability to directly compare damage in the WM and GM. The striking difference in the extent of inflammation between the WM and GM allows investigation of mechanisms of myelin damage, axonal damage and inflammation in MS (19). Furthermore, regional differences in the surface expression of several important neuroimmunological molecules on microglia from mice (31) indicate distinct microglia populations. Several lines of evidence suggest that the most distinct differences between the microglia populations are found in the WM and GM, including (but not restricted to) the corpus callosum and the cerebral cortex, respectively. Next to the evident morphological disparities, WM and GM microglia are known to be differentially affected by brain ageing, show differences in the cellular expression levels of several activation markers under physiological conditions and contribute to a different inflammatory milieu in WM versus GM lesions in demyelinating disorders. Therefore, differences between microglia residing in the WM and GM might explain the differences observed in leukocortical lesions regarding inflammation. We have shown that phagocytosis of neuronal antigens occurs in active and chronic active WM MS lesions (17). However, whether phagocytosis of neuronal debris occurs in GM lesions is as yet unknown.

In WM MS lesions axonal damage correlates with the degree of inflammation (2-5, 17). Although inflammation might contribute to axonal damage, inflammation in the GM is not as extensive as in the WM but damage is clearly present (2, 19). To investigate these findings we compared the GM and WM part of leukocortical lesion and confirmed higher levels of inflammation in the WM part compared to the GM part of the lesions. However, this difference was not clear in the extent of axonal damage. This might indicate that in the GM, activated microglia are more toxic or other mechanisms contribute to axonal damage. Axons in the GM might be more vulnerable to environmental changes as well since these axons are not fully myelinated. Therefore, little inflammation present in the GM may have a greater impact than in the WM. Since we did not observe a correlation between axonal damage and the number of HLA-DR$^+$ cells in the GM, different mechanisms most likely contribute to axonal damage in the GM. One possibility might be the production and secretion of toxic molecules by HLA-DR$^+$ cells influencing axonal integrity and causing axonal damage in the GM (2, 6, 9). The observed axonal damage in the GM without apparent inflammation might also be a result of retrograde degeneration (33). Although still a subject of debate, meningeal inflammation has been implicated in cortical pathology (34-37), but it is still unclear whether a relation between meningeal infiltrates and leukocortical lesions exists. In the paraffin blocks we included in this study, meningeal tissue was not present.

Despite the fact that the nature of the relationship between microglia morphology and state of activation still awaits elucidation, one of the most widely accepted signs of microglia activation is their transformation from highly ramified to rounded cells, accompanied by gradual shortening and thickening of the processes. We observed significant differences between WM and GM microglia in respect of the length, volume and the number of branching points of their processes, confirming the earlier subjective observations regarding their morphological differences (38). WM microglia had consistently fewer and less ramified processes than GM microglia, which might point towards a different state of activation. To investigate whether, as suggested by their morphological differences, WM and GM microglia exist at

a different state of activation, we performed a genome wide mRNA expression analysis of the two microglia populations from mice. For most of the genes, normalised gene expression levels were generally very low in both WM and GM microglia. Nonetheless, microarray analysis of gene expression revealed more than two thousand genes that were significantly differentially expressed between WM and GM microglia. Many of these differentially expressed genes belong to pathways involved in neuroimmunological processes, such as the Toll-like receptor pathway and the antigen processing and presentation pathway. However, most of the differences observed at the gene expression level were small (less than fivefold difference in the normalised expression levels) and were not apparent at the protein level under physiological conditions. On the contrary, WM and GM microglia that were systemically challenged with LPS in an endotoxin model showed moderate differences in the induction of some of the co-stimulatory molecules and MHCII. This up regulation is in line with other reports showing induced expression of genes upon exposure to different stimuli (31, 32, 39). The fact that we could, with a highly sensitive technique, detect differences at the gene expression level between corpus callosum and cortex resident microglia, which could not be identified at the protein level under physiological conditions, but were (to some extent) confirmed upon peripheral LPS challenge, might highlight the possibility that the true nature of the differences between these populations would manifest themselves under the state of compromised CNS homeostasis.

One of the major characteristics of microglia is phagocytosis of debris, suggested to be essential for regeneration in neurological deficits (40-43). Phagocytosis of APP^+ structures by HLA-DR^+ cells was significantly more frequent in the WM compared with the GM in leukocortical MS lesions. However, in time-lapse experiments with acutely isolated mouse microglia *in vitro* we did not observe distinct differences in phagocytic capacity between microglia from cortex or corpus callosum. Similar phagocytic capacity was also observed in human microglia derived from WM and GM post-mortem tissue (preliminary data, not shown). The nature of the debris and local environment in which microglia phagocytose might be important in regulating clearance of debris (44-46). Moreover, the contribution of phagocytosis of neuronal antigens could influence the nature of the microglia and macrophages present. Previous studies showed that phagocytosis of myelin induces an anti-inflammatory phenotype in macrophages (46). Preliminary studies with human microglia derived from WM brain tissue showed a trend in up regulated gene expression of the pro-inflammatory cytokine IL-17 and anti-inflammatory cytokine TGFβ 1 h after phagocytosis of human WM debris compared to human GM debris. It is likely that the local environment is of importance in induction of immune responses, since recently it is shown that in the cuprizone animal model, where demyelination is induced in both WM and GM, mRNA levels of the chemoattractants CCL2 and CCL3 are less expressed in the GM compared to the WM (47). One of the explanations of less microglia activation in the GM is the presence of less myelin compared to the WM (18). Clarner and colleagues show that stereotactic injection of myelin in the cortex and corpus callosum in mice leads to similar microglia activation in both regions. Because our focus is more on axonal damage in WM and GM, we injected neuronal debris in the cortex and corpus callosum of mice and also observed similar activation of $Iba1^+$ cells in these regions. Although we did not investigate the origin of these $Iba1^+$ cells, this result indicates that acute axonal damage can activate microglia in WM and GM.

In conclusion, functional differences between HLA-DR^+ cells in the GM and the WM

might be responsible for the extent of axonal damage observed in the GM part of leukocortical MS lesions, despite the lower degree of inflammation compared with the WM.

Acknowledgements
We thank Kamilla Kutzlibay (Aachen) for the assistance with stereotactic injections. We thank Dr. Malika Bsibsi (Delta Crystallon BV, Leiden, The Netherlands) for assistance with experiments on human microglia. We also thank Jaap van Veldhuizen en Ron Otsen (Pathology, VUmc) for their assistance with photomicroscopy.

Financial Support
This work was supported by the Dutch Stichting MS Research (grant 07-627).

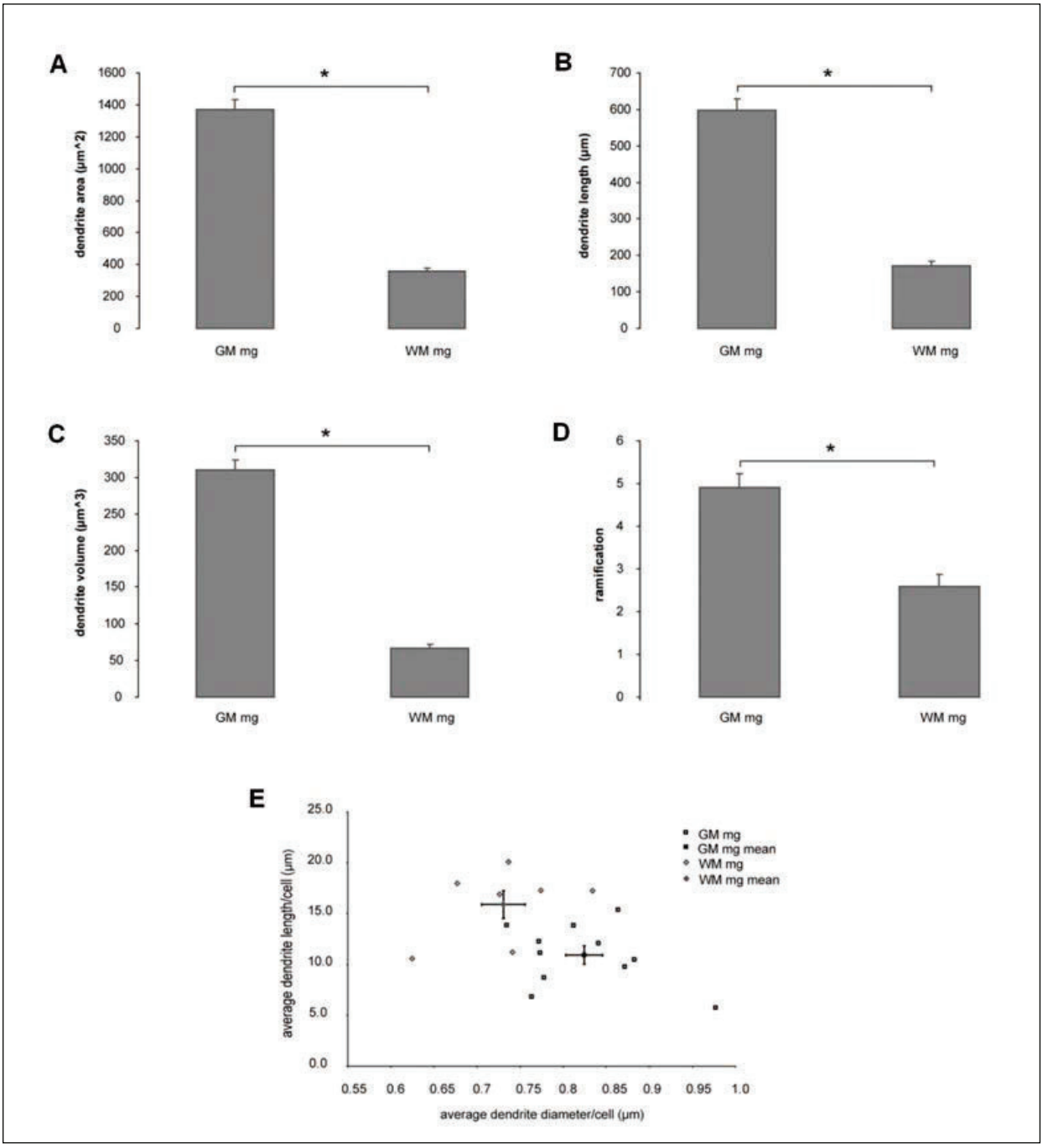

Supplementary Figure 1. Significant differences in cell morphology between microglia residing in the CNS white and grey matter. *(**A-D**) The total dendrite area per cell, the total dendrite length per cell, the total dendrite volume per cell and the total number of ramification points per cell is plotted for WM and GM microglia, respectively. **E**) The average dendrite diameter per cell is plotted against the average dendrite length per cell. Error bars in B-F represent the standard error of the mean (SEM). n=10 for both WM and GM microglia. * p<0,001; GM mg, grey matter microglia; WM mg, white matter microglia. See figure on the previous page.*

References

1. Trapp, B.D., Ransohoff, R., and Rudick, R. 1999. Axonal pathology in multiple sclerosis: relationship to neurologic disability. *Curr Opin Neurol* 12:295-302.
2. Trapp, B.D., and Nave, K.A. 2008. Multiple sclerosis: an immune or neurodegenerative disorder? *Annu Rev Neurosci* 31:247-269.
3. Trapp, B.D., Peterson, J., Ransohoff, R.M., Rudick, R., et al. 1998. Axonal transection in the lesions of multiple sclerosis. *N Engl J Med* 338:278-285.
4. Ferguson, B., Matyszak, M.K., Esiri, M.M., and Perry, V.H. 1997. Axonal damage in acute multiple sclerosis lesions. *Brain* 120 (Pt 3):393-399.
5. Bitsch, A., Schuchardt, J., Bunkowski, S., Kuhlmann, T., and Bruck, W. 2000. Acute axonal injury in multiple sclerosis. Correlation with demyelination and inflammation. *Brain* 123 (Pt 6):1174-1183.
6. Griffiths, I., Klugmann, M., Anderson, T., Yool, D., et al. 1998. Axonal swellings and degeneration in mice lacking the major proteolipid of myelin. *Science* 280:1610-1613.
7. Nikic, I., Merkler, D., Sorbara, C., Brinkoetter, M., et al. 2011. A reversible form of axon damage in experimental autoimmune encephalomyelitis and multiple sclerosis. *Nat Med* 17:495-499.
8. Brown, G.C., and Borutaite, V. 2002. Nitric oxide inhibition of mitochondrial respiration and its role in cell death. *Free Radic Biol Med* 33:1440-1450.
9. Amor, S., and Huizinga, R. 2011. Autoimmunity to Neuronal Proteins in Neurological Disorders: *Nova Science Publishers Inc*
10. Huizinga, R., Hintzen, R.Q., Assink, K., van Meurs, M., and Amor, S. 2009. T-cell responses to neurofilament light protein are part of the normal immune repertoire. *Int Immunol* 21:433-441.
11. Silber, E., Semra, Y.K., Gregson, N A., and Sharief, M.K. 2002. Patients with progressive multiple sclerosis have elevated antibodies to neurofilament subunit. *Neurology* 58:1372-1381.
12. Mathey, E.K., Derfuss, T., Storch, M.K., Williams, K.R., et al. 2007. Neurofascin as a novel target for autoantibody-mediated axonal injury. *J Exp Med* 204:2363-2372.
13. Forooghian, F., Cheung, R.K., Smith, W.C., O'Connor, P., and Dosch, H.M. 2007. Enolase and arrestin are novel nonmyelin autoantigens in multiple sclerosis. *J Clin Immunol* 27:388-396.
14. Zhang, Y., Da, R.R., Guo, W., Ren, H.M., et al. 2005. Axon reactive B cells clonally expanded in the cerebrospinal fluid of patients with multiple sclerosis. *J Clin Immunol* 25:254-264.
15. Huizinga, R., Gerritsen, W., Heijmans, N., and Amor, S. 2008. Axonal loss and gray matter pathology as a direct result of autoimmunity to neurofilaments. *Neurobiol Dis* 32:461-470.
16. Huizinga, R., Heijmans, N., Schubert, P., Gschmeissner, S., et al. 2007. Immunization with neurofilament light protein induces spastic paresis and axonal degeneration in Biozzi ABH mice. *J Neuropathol Exp Neurol* 66:295-304.

17. Huizinga, R., van der Star, B.J., Kipp, M., Jong, R., et al. 2012. Phagocytosis of neuronal debris by microglia is associated with neuronal damage in multiple sclerosis. *Glia* 60:422-431.
18. Clarner, T., Diederichs, F., Berger, K., Denecke, B., et al. 2012. Myelin debris regulates inflammatory responses in an experimental demyelination animal model and multiple sclerosis lesions. *Glia* 60:1468-1480.
19. Peterson, J.W., Bo, L., Mork, S., Chang, A., and Trapp, B.D. 2001. Transected neurites, apoptotic neurons, and reduced inflammation in cortical multiple sclerosis lesions. *Ann Neurol* 50:389-400.
20. Carson, M.J., Bilousova, T.V., Puntambekar, S.S., Melchior, B., et al. 2007. A rose by any other name? The potential consequences of microglial heterogeneity during CNS health and disease. *Neurotherapeutics* 4:571-579.
21. Alldinger, S., Wunschmann, A., Baumgartner, W., Voss, C., and Kremmer, E. 1996. Up-regulation of major histocompatibility complex class II antigen expression in the central nervous system of dogs with spontaneous canine distemper virus encephalitis. *Acta Neuropathol* 92:273-280.
22. Gehrmann, J., Banati, R.B., and Kreutzberg, G.W. 1993. Microglia in the immune surveillance of the brain: human microglia constitutively express HLA-DR molecules. *J Neuroimmunol* 48:189-198.
23. Ogura, K., Ogawa, M., and Yoshida, M. 1994. Effects of ageing on microglia in the normal rat brain: immunohistochemical observations. *Neuroreport* 5:1224-1226.
24. Ong, W.Y., Leong, S.K., Garey, L.J., Tan, K.K., and Zhang, H.F. 1995. A light and electron microscopic study of HLA-DR positive cells in the human cerebral cortex and subcortical white matter. *J Hirnforsch* 36:553-563.
25. Sasaki, A., and Nakazato, Y. 1992. The identity of cells expressing MHC class II antigens in normal and pathological human brain. *Neuropathol Appl Neurobiol* 18:13-26.
26. Sheffield, L.G., and Berman, N.E. 1998. Microglial expression of MHC class II increases in normal aging of nonhuman primates. *Neurobiol Aging* 19:47-55.
27. Styren, S.D., Civin, W.H., and Rogers, J. 1990. Molecular, cellular, and pathologic characterization of HLA-DR immunoreactivity in normal elderly and Alzheimer's disease brain. *Exp Neurol* 110:93-104.
28. Kullberg, S., Aldskogius, H., and Ulfhake, B. 2001. Microglial activation, emergence of ED1-expressing cells and clusterin upregulation in the aging rat CNS, with special reference to the spinal cord. *Brain Res* 899:169-186.
29. De Groot, C.J., Bergers, E., Kamphorst, W., Ravid, R., et al. 2001. Post-mortem MRI-guided sampling of multiple sclerosis brain lesions: increased yield of active demyelinating and (p)reactive lesions. *Brain* 124:1635-1645.
30. Bo, L., Geurts, J.J., Ravid, R., and Barkhof, F. 2004. Magnetic resonance imaging as a tool to examine the neuropathology of multiple sclerosis. *Neuropathol Appl Neurobiol* 30:106-117.
31. De Haas, A.H., Boddeke, H.W., and Biber, K. 2008. Region-specific expression of immunoregulatory proteins on microglia in the healthy CNS. *Glia* 56:888-894.
32. Olah, M., Ping, G., De Haas, A.H., Brouwer, N., et al. 2009. Enhanced hippocampal neurogenesis in the absence of microglia T cell interaction and microglia activation in the murine running wheel model. *Glia* 57:1046-1061.
33. Balk, L.J., Twisk, J.W., Steenwijk, M.D., Daams, M., et al. 2014. A dam for retrograde axonal degeneration in multiple sclerosis? *J Neurol Neurosurg Psychiatry*.
34. Choi, S.R., Howell, O.W., Carassiti, D., Magliozzi, R., et al. 2012. Meningeal inflammation plays a role in the pathology of primary progressive multiple sclerosis.

Brain 135:2925-2937.
35. Howell, O.W., Reeves, C.A., Nicholas, R., Carassiti, D., et al. 2011. Meningeal inflammation is widespread and linked to cortical pathology in multiple sclerosis. *Brain* 134:2755-2771.
36. Kooi, E.J., van Horssen, J., Witte, M.E., Amor, S., et al. 2009. Abundant extracellular myelin in the meninges of patients with multiple sclerosis. *Neuropathol Appl Neurobiol* 35:283-295.
37. Magliozzi, R., Howell, O., Vora, A., Serafini, B., et al. 2007. Meningeal B-cell follicles in secondary progressive multiple sclerosis associate with early onset of disease and severe cortical pathology. *Brain* 130:1089-1104.
38. Lawson, L.J., Perry, V.H., Dri, P., and Gordon, S. 1990. Heterogeneity in the distribution and morphology of microglia in the normal adult mouse brain. *Neuroscience* 39:151-170.
39. Trudler, D., Farfara, D., and Frenkel, D. 2010. Toll-like receptors expression and signaling in glia cells in neuro-amyloidogenic diseases: towards future therapeutic application. *Mediators Inflamm.*
40. Filbin, M.T. 2003. Myelin-associated inhibitors of axonal regeneration in the adult mammalian CNS. *Nat Rev Neurosci* 4:703-713.
41. Neumann, H., Kotter, M.R., and Franklin, R.J. 2009. Debris clearance by microglia: an essential link between degeneration and regeneration. *Brain* 132:288-295.
42. Makranz, C., Cohen, G., Baron, A., Levidor, L., et al. 2004. Phosphatidylinositol 3-kinase, phosphoinositide-specific phospholipase-Cgamma and protein kinase-C signal myelin phagocytosis mediated by complement receptor-3 alone and combined with scavenger receptor-AI/II in macrophages. *Neurobiol Dis* 15:279-286.
43. Reichert, F., and Rotshenker, S. 2003. Complement-receptor-3 and scavenger-receptor-AI/II mediated myelin phagocytosis in microglia and macrophages. *Neurobiol Dis* 12:65-72.
44. Sospedra, M., and Martin, R. 2005. Immunology of multiple sclerosis. *Annu Rev Immunol* 23:683-747.
45. Van Rossum, D., and Hanisch, U.K. 2004. Microglia. *Metab Brain Dis* 19:393-411.
46. Boven, L.A., Van Meurs, M., Van Zwam, M., Wierenga-Wolf, A., et al. 2006. Myelin-laden macrophages are anti-inflammatory, consistent with foam cells in multiple sclerosis. *Brain* 129:517-526.
47. Buschmann, J.P., Berger, K., Awad, H., Clarner, T., et al. 2012. Inflammatory response and chemokine expression in the white matter corpus callosum and gray matter cortex region during cuprizone-induced demyelination. *J Mol Neurosci* 48:66-76.